Carbonic Anhydrase Inhibitors: Hypoxia-Activatable Sulfonamides Incorporating Disulfide Bonds that Target the Tumor-Associated Isoform IX†

Giuseppina De Simone,*,‡ Rosa Maria Vitale,‡ Anna Di Fiore,‡ Carlo Pedone,‡,§ Andrea Scozzafava,# Jean-Louis Montero,|| Jean-Yves Winum,|| and Claudiu T. Supuran*,#

Istituto di Biostrutture e Bioimmagini−CNR, Via Mezzocannone 16, 80134 Naples, Italy, Dipartimento delle Scienze Biologiche-Sezione Biostrutture, University of Naples "Federico II", Via Mezzocannone 16, 80134 Naples, Italy, Polo Scientifico, Laboratorio di Chimica Bioinorganica, Rm. 188, Università degli Studi di Firenze, Via della Lastruccia 3, 50019 Sesto Fiorentino, Florence, Italy, and Laboratoire de Chimie Biomoléculaire, UMR 5032, Ecole Nationale Supérieure de Chimie de Montpellier, Université Montpellier II, 8 Rue de l'Ecole Normale, 34296 Montpellier Cedex, France

Received May 8, 2006

An approach for designing bioreductive, hypoxia-activatable carbonic anhydrase (CA, EC 4.2.1.1) inhibitors targeting the tumor-associated isoforms is reported. Sulfonamides incorporating 3,3′-dithiodipropionamide/2,2′-dithiodibenzamido moieties were prepared and reduced enzymatically/chemically in conditions present in hypoxic tumors, leading to thiols. The X-ray crystal structure of the most promising compound, 4-(2-mercaptophenylcarboxamido)benzenesulfonamide, which as disulfide showed a K_I against hCA IX of 653 nM (in reduced form of 9.1 nM), in adduct with hCA II showed the inhibitor making favorable interactions with Gln92, Val121, Phe131, Leu198, Thr199, Thr200, Pro201, and Pro202, whereas the sulfamoyl moiety was coordinated to the Zn^{2+} ion. The same interactions were preserved in the adduct with hCA IX, but in addition, a hydrogen bond between the SH moiety of the inhibitor and the amide nitrogen of Gln67 was evidenced, which may explain the almost 2 times more effective inhibition of the tumor-associated isozyme over the cytosolic isoform.

Introduction

Hypoxia and acidic extracellular pH_e constitute hallmarks of many solid tumors because of their improperly built and insufficiently functioning vasculature, lack of oxygen, and unregulated functioning of house-keeping enzymes, among which are the carbonic anhydrases (CAs, EC 4.2.1.1) involved in pH homeostasis, ion transport, and biosynthetic processes.[1−3] Wykoff et al.[3a] investigated the expression of the CA9 gene,[4] which encodes a tumor-associated CA isozyme, i.e., CA IX, in response to hypoxia. This research was based on observations showing that the von Hippel Lindau tumor suppressor protein (pVHL), which functions as a recognition component of the E3 ubiquitin ligase complex, negatively regulates the stability of the α subunit of the hypoxia inducible factor 1α (HIF-1α) in the presence of O_2.[5] Under normoxic conditions, oxygen-dependent prolyl hydroxylases (PHDs) hydroxylate HIF-1α at specific proline residues in the central oxygen-dependent degradation domain.[6] This hydroxylation mediates the interaction between HIF-1α and pVHL, leading to the degradation of HIF-1α.[7,8] Under hypoxic conditions, which often develop in tumors,[1] the lack of oxygen does not allow PHDs to hydroxylate HIF-1α and thus interferes with pVHL recognition pathways. In this way, HIF-1α accumulates in the cell and interacts with a constitutive HIF-β subunit to form an active HIF-1 transcription factor that binds a hypoxia response elements (HRE) in the promoters of many hypoxia-regulated genes, activating their expression.[6−8] By this mechanism, hypoxic tumor cells can induce a number of genes involved in their adaptation to low oxygen concentrations, including those regulating cell survival, proliferation, apoptosis, angiogenesis, and glucose metabolism.[9,10] Wykoff et al.[3a] showed that the CA9 promoter contains a functional HRE element localized on an antisense strand that is highly responsive to hypoxia, possibly because of its vicinity to a transcription start site, thus making CA9 one the most strongly hypoxia-induced genes.[1,3,9,10] As a consequence, hypoxic tumors overexpress massive amounts of CA IX, an enzyme possessing high catalytic activity for the hydration of CO_2 to bicarbonate and protons, which is also inhibited by the classical CA inhibitors belonging to the sulfonamide, sulfamate, and sulfamide classes of compounds.[1,11−15]

It has been proved by our groups that CA IX is a druggable target, being inhibited in the low nanomolar range by many different classes of sulfonamides, sulfamates, and sulfamides.[11−15] In addition, Svastova et al.[11] showed that in different tumor cell cultures in which CA IX is inhibited by potent and selective sulfonamide inhibitors, pH_e returns to a more normal range (for example, from a pH value of 6.4 in the initial tumor cell culture to a pH of 7.2 after CA IX inhibition with sulfonamides)[11] accompanied by an enhanced apoptosis of the tumor cells. Correlated with the fact that it has been shown earlier that some CA inhibitors do show anticancer activity in vivo,[16−18] CA IX inhibition may constitute an attractive new approach for the management of hypoxic tumors, which are generally nonresponsive to the classical radio- and chemotherapy.[1−3]

One approach for improving the selectivity of tumor cell killing by anticancer drugs consists of the use of less toxic prodrugs that can be selectively activated in the tumor tissue, exploiting some unique aspects of tumor physiology such as selective enzyme expression or hypoxia.[19] As mentioned above, since CA IX is overexpressed in hypoxic tumors, being present in very low amounts only in some parts of the normal gastrointestinal tract, this enzyme may constitute an attractive target for the design of hypoxia-activatable prodrugs. In fact,

†Coordinates and structure factors have been deposited in the Brookhaven Protein Data Bank (accession code 2HD6).

* To whom correspondence should be addressed. For G.D.S.: phone, +39-081-2534579; fax, +39-081-2536642; e-mail, gdesimon@unina.it. For C.T.S.: phone, +39-055-4573005; fax, +39-055-4573385; e-mail, claudiu.supuran@unifi.it.

‡ Istituto di Biostrutture e Bioimmagini−CNR.

§ University of Naples "Federico II".

Università degli Studi di Firenze.

|| Université Montpellier II.

10.1021/jm060531j CCC: $33.50
Published on Web 08/10/2006

there are many examples in the literature regarding bioreductive prodrugs, which use the reduction of quinones, *N*-oxides, and nitroaromatics by endogenous enzymes or radiation, the cleavage of amides by endogenous peptidases, and hydrolytic metabolism by a variety of exogenous enzymes, including phosphatases, kinases, amidases, and glycosidases,[19−23] but no CA inhibitors were designed until now for this type of application. Here, we report the first hypoxia-activatable prodrugs targeting CA IX, an isozyme abundantly overexpressed in hypoxic tumors, an X-ray crystal structure of one of the most promising of such agents with the physiologically relevant isozyme CA II, as well as modeling binding studies of this compound with the target isoform, the transmembrane, and tumor-associated CA IX.

Results and Discussion

Chemistry. The rationale for the design of hypoxia-activatable prodrugs targeting the tumor-associated CA IX is based on exploiting the reducing conditions present in such tumors, in which pO_2 is generally less than 1%.[19d] Thus, we considered the design of disulfide derivatives of the main class of CA inhibitors, the aromatic/heteroaromatic sulfonamides.[24] In principle, such disulfide-containing sulfonamides should be bulky enough and thus unable to bind within the restricted space of the CA active site, which normally can accommodate only one benzenesulfonamide/heterocyclic sulfonamide moiety.[15] However, bioreduction in hypoxic tumors of such dimeric sulfonamides, eventually mediated by the redox protein thioredoxin-1, which is found at high levels in many human cancers which is known to mediate this type of reduction,[25] would generate thiols that are much less bulky and thus in principle should bind better to the active site of the CA isoforms present in tumor tissues. Since CA IX is mainly found only in hypoxic tumors, this type of hypoxia-activatable prodrug will be formed only in the cancer tissue, and as a consequence, no monomeric sulfonamide derivative should be present outside the tumor cell. This may lead to a tumor-specific drug with potentially fewer side effects due to inhibition of other CA isoforms highly abundant in noncancer tissues, such as CA I, II, IV, or VA.[24]

The chemistry employed for the design of the new compounds reported here is shown in Scheme 1. A series of 3,3′-dithiodipropionamide sulfonamides (**2a**−**d**, **3**, and **4**) were prepared starting from the commercially available dithiodipropionic acid, which was converted to 3,3′-dithiodipropionyl dichloride (**1**) with neat thionyl chloride. The acyl chloride **1** was then reacted with the corresponding aminosulfonamide (i.e., sulfanilamide, 4-aminoethylbenzenesulfonamide, 3-halogenated sulfanilamides, 5-amino-1,3,4-thiadiazole-2-sulfonamide, or 4-methyl-5-imino-δ^2-1,3,4-thiadiazoline-2-sulfonamide)[26] in pyridine/dioxane, leading to the compounds **2**−**4** in good yields, as reported earlier for structurally related carboxamidosulfonamides[26] (Scheme 1).

The disulfide benzamide compounds **5a** and **5b** were synthesized as previously described by Turpin et al.[27] by reacting sulfanilamide or 4-aminoethylbenzenesulfonamide with 2,2′-dithiodibenzoyl chloride. These two derivatives have been reported earlier as possible anti-HIV agents that provoke metal extrusion from the zinc fingers of the viral nucleocapsid.[27]

The reduced derivatives of disulfides **2**−**5** (designated as **H2**−**H5**; see discussion later in the text and Scheme 2) have been prepared by in situ reduction of the disulfides with a stoichiometric amount of aqueous sodium dithionite directly in the enzyme assay system (dithionite is not a CA I, II, or IX inhibitor)[28] and were not isolated as pure compounds, since just the prodrugs **2**−**5** are of interest for possible new antitumor therapies.

Scheme 1

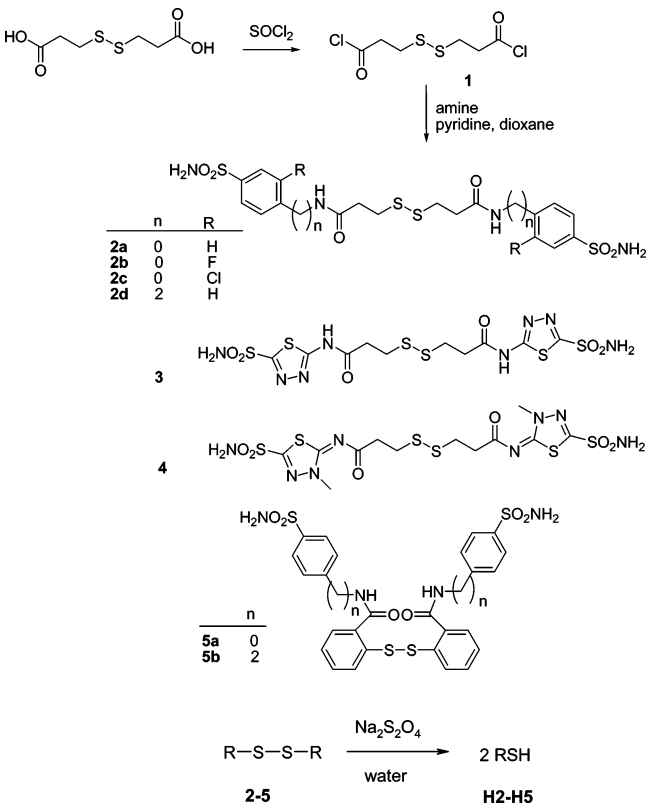

Scheme 2

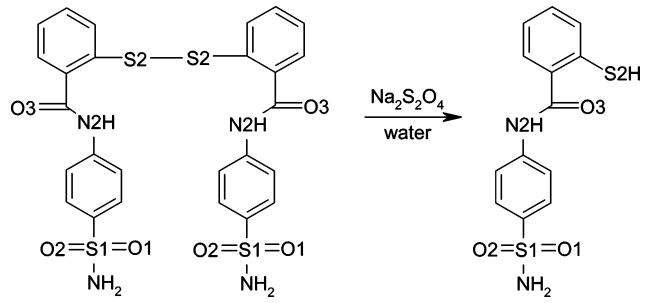

CA Inhibition. Derivatives **2**−**5** reported here, their reduced monomeric thiols **H2**−**H5**, and standard, clinically used[24] sulfonamide CA inhibitors, such as acetazolamide AAZ, methazolamide MZA, ethoxzolamide EZA, dichlorophenamide DCP, zonisamide ZNS, sulpiride SLP and indisulam IND, were

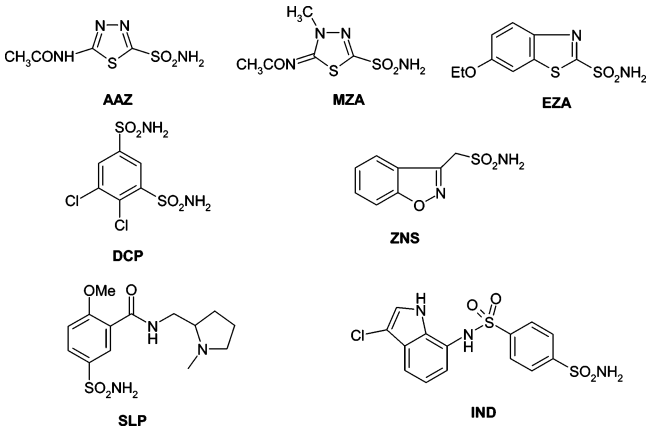

assayed[29] for the inhibition of three physiologically/pharmacologically relevant CA isozymes: the ubiquitous cytosolic

Table 1. Inhibition of CA Isoforms I, II, and IX with Disulfides **2**−**5**, the Corresponding Reduced Thiols **H2**−**H5**, and the Standard Sulfonamide CA Inhibitors AAZ, MZA, EZA, DCP, ZNS, SLP, and IND

	K_I [a] (nM)			selectivity ratio
compd	hCA I[b]	hCA II[b]	hCA IX[c]	hCA II/hCA IX
2a	97	94	78	1.20
H2a	74	27	65	0.41
2b	69	64	79	0.81
H2b	18	9.7	15	0.64
2c	71	39	72	0.54
H2c	10	8.9	8.7	1.02
2d	5115	71	71	1.00
H2d	275	24	56	0.42
3	60	61	18	3.38
H3	17	9.1	3.6	2.52
4	41	42	9.3	4.51
H4	9.5	9.3	3.2	2.90
5a	4350	4975	653	7.61
H5a	276	16	9.1	1.75
5b	4265	4860	724	6.71
H5b	85	29	9.0	3.22
AAZ	250	12	25	0.48
MZA	50	14	27	0.51
EZA	25	8	34	0.23
DCP	1200	38	50	0.76
ZNS	56	35	5	7.00
SLP	1200	40	31	1.29
IND	31	15	24	0.62

[a] Errors in the range 5−10% of the reported value (from three different assays). [b] Human recombinant isozymes, stopped-flow CO_2 hydrase assay method.[29] [c] Catalytic domain of the human, recombinant enzyme, stopped-flow CO_2 hydrase assay method.[29]

isoforms hCA I and II (h means isozyme of human origin) and the transmembrane, tumor-associated isozyme hCA IX (Table 1). The following SAR was observed from data of Table 1.

(i) Against the slow cytosolic isozyme hCA I, derivatives **2d**, **5a**, and **5b** showed weak inhibitory activity, with inhibition constants (K_I) in the range 4265−5115 nM. On the other hand, derivatives **2a**, **H2a**, **2b**, **H2d**, **3**, **4**, **H5a**, and **H5b** were much more potent hCA I inhibitors, with K_I values in the range 41−276 nM. The best hCA I inhibitors were **H2b**, **H2c**, **H3**, and **H4**, which showed K_I values in the low nanomolar range of 9.5−18 nM, being much more effective in inhibiting this isozyme than ethoxzolamide (one of the best hCA I inhibitors reported)[24] and the other clinically used derivatives. It is observed that all the reduced compounds are much more inhibitory compared to the corresponding dimeric disulfides. Another observation is that the derivatives incorporating the bulky 2,2′-dithiodibenzamido moiety (**5a**, **5b**) were generally less active as hCA I inhibitors compared to the compounds incorporating the less bulky, aliphatic disulfide moiety 3,3′-dithiodipropionamide. An exception is **2d**/**H2d**, which showed a behavior similar to that of the aromatic disulfide containing sulfonamides **5a** and **5b** (and of their reduced counterparts, of course). For the 3,3′-dithiodipropionamides **2**−**4**, the presence of halogen atoms in the sulfanilamide scaffold or the heteroaromatic rings from **3** and **4** leads to enhanced hCA I inhibitory activity compared to that of the parent sulfanilamide **2a** (this is also valid for the corresponding reduced derivatives of the disulfides discussed above).

(ii) Against the rapid, pharmacologically highly relevant isoform hCA II, the compounds investigated here also showed very interesting inhibitory activity. Thus, as for the previously discussed isoform, the disulfide benzamide compounds **5a** and **5b** showed very weak inhibitory activity, with K_I values in the range 4860−4975 nM. In contrast, the corresponding reduced derivatives **H5a** and **H5b** (as well as all the other reduced compounds **H2**−**H4** investigated here) showed effective hCA II inhibitory activity, with K_I values in the range 8.9−29 nM. The other disulfides, incorporating aliphatic moieties, of types **2a**−**d**, **3**, and **4** showed an inhibitory activity between those discussed above. These compounds were less inhibitory compared to the corresponding thiols, with K_I values in the range 42−94 nM, but much more effective inhibitors compared to **5a** and **5b**. Thus, our hypothesis that bulky disulfides such as compounds **2**−**5** reported here may show a hindered access to the CA active site due to steric impairment may be true. It is also noted that the clinically used compounds AAZ, MZA, EZA, DCP, ZNS, SLP, and IND are generally quite potent inhibitors of this isozyme, with K_I values in the range 8−40 nM.

(iii) Against the tumor-associated isoform hCA IX, the aromatic disulfides **5a** and **5b** again showed weak inhibitory activity (K_I values in the range 653−724 nM), whereas derivatives **2a**, **H2a**, **2b**, **2c**, **2d**, and **H2d** were medium-potency inhibitors (K_I values in the range 56−79 nM). On the other hand, the other reduced derivatives, i.e., **H2b**, **H2c**, **H3** (and also the disulfide **3**), **H4** and its disulfide **4**, **H5a**, and **H5b**, were very potent hCA IX inhibitors, with inhibition constants in the range 3.2−18 nM, in the same range as the clinically used compounds AAZ, MZA, EZA, DCP, ZNS, SLP, and IND (Table 1). It is observed that for the 3,3′-dithiodipropionamide sulfonamides, the difference in hCA IX inhibitory activity between the reduced and the corresponding oxidized form is not very important. The monomeric, reduced (thiol) form is always more inhibitory compared with the disulfide (dimeric) syulfonamide. This difference is very high in the case of the disulfide benzamide compounds **5a** and **5b** (the case in which the reduced forms **H5a** and **H5b** are 72−80 times more inhibitory compared to the corresponding disulfide). Thus, considering the fact that for these two derivatives the difference between the hCA IX (but also hCA II and I) inhibitory activity of the reduced and oxidized forms is the highest one and also that the two compounds (in reduced form) are very potent hCA IX inhibitors, we consider them interesting candidates for in vivo evaluation as potential bioreductive drugs. As a consequence, we chose one of these derivatives (**5a**) for detailed X-ray crystallographic and modeling studies in order to better understand its interaction with various CA isozymes.

(iv) Since hCA II is a ubiquitous house-keeping enzyme present in high amounts in many tissues/cells, it is important to discuss the selectivity ratios of the new compounds **2**−**5** for the inhibition of the target enzyme (hCA IX) over hCA II (Table 1). Indeed, many of the synthesized compounds are better hCA II inhibitors than hCA IX inhibitors, with a selectivity ratio of <1 (e.g., **H2a**, **2b**, **H2b**, **2c**, **H2d**, and all the clinically used sulfonamides except ZNS and SLP). However, some of the new derivatives reported here, such as **2a**, **H2c**, **2d**, and **H5a**, show selectivity ratios above unity, in the range 1.00−1.75. Several other new derivatives, such as **3**, **H3**, **4**, **H4**, **5a**, **5b**, and **H5b** show selectivity ratios in the range 2.52−7.61, thus showing a certain degree of selectivity for the inhibition of the tumor-associated over the cytosolic isozymes. Considering that the disulfide **5a** is a very weak hCA I, II, and IX inhibitor, whereas the corresponding reduced form **H5a** is a potent and slightly isozyme-IX-selective inhibitor, we chose this compound for X-ray crystallographic and modeling studies.

X-ray Crystallography. To determine the key interactions and molecular features that contribute to the inhibitory properties of the most promising derivative identified here as a potential bioreductive antitumor compound, i.e., 4-(2-mercaptophenylcarboxamido)benzenesulfonamide **H5a** (see Scheme 2 for the

Table 2. Crystal Parameters, Data Collection, and Refinement Statistics for the HCA II−**H5a** Complex[a]

crystal parameters	
space group	$P2_1$
a (Å)	42.07
b (Å)	41.26
c (Å)	71.66
β (deg)	104.28
data collection statistics (20.00−1.80 Å)	
temp (K)	100
total reflections	68 934
unique reflections	21 376
completeness (%)	96.0 (86.2)
R_{sym} [b]	0.055 (0.210)
mean *I* (*σ*(I))	18.5 (4.7)
refinement statistics (20.00−1.80 Å)	
R factor [c] (%)	18.4
R_{free} [c] (%)	21.8
rmsd from ideal geometry	
bond length (Å)	0.005
bond angle (deg)	1.3
no. of protein atoms	2071
no. of inhibitor atoms	41
no. of water molecules	230
average *B* factor (Å^2)	13.5

[a] Values in parentheses refer to the highest resolution shell. [b] $R_{sym} = \sum|I_i - \langle I\rangle|/\sum I_i$; over all reflections. [c] *R* factor $= \sum|F_o - F_c|/\sum F_o$; R_{free} calculated with 5% of data withheld from refinement.

crystallographic numbering of the atoms in this derivative and its disulfide prodrug), this compound has been cocrystallized with hCA II (trials to crystallize hCA IX in our and other laboratories were unsuccessful until now). Crystals of the adduct are isomorphous with those of the native protein,[30] allowing for the determination of the crystallographic structure by difference Fourier techniques. The structure has been refined using the CNS program[31] to a crystallographic *R* factor of 18.4% and an R_{free} of 21.8% in the 20.00−1.80 Å resolution range. The refined structure represents a good geometry with rmsd values from ideal bond lengths and angles of 0.005 Å and 1.3°, respectively. The average temperature factor (*B*) for all atoms is 13.5 Å^2. The overall quality of the model is excellent with all residues in the allowed regions of the Ramachandran plot. Refinement statistics are summarized in Table 2. Inspection of the electron density maps at various stages of the refinement showed features compatible with the presence of only one **H5a** molecule bound to the active site (Figure 1). These maps are well defined for the 4-aminocarbonylbenzenesulfonamide moiety of the inhibitor. A poorer definition is observed for the 2-mercaptophenyl functionality, suggesting a greater flexibility of this group within the hCA II active site. The structure of hCA II in the enzyme−inhibitor complex exhibited only minor differences when compared to that of the native protein,[30] as shown by the rmsd calculated over all the Cα atoms between the hCA II−**H5a** complex and the unbound enzyme (rmsd = 0.37 Å). Interactions between the protein and Zn^{2+} ion were entirely preserved in the adduct. A careful analysis of the three-dimensional structure of the complex revealed a compact binding between the inhibitor and the enzyme active site, with the tetrahedral geometry of the Zn^{2+} binding site and the key hydrogen bonds between the sulfonamide moiety of the inhibitor and enzyme active site all retained with respect to other hCA II−sulfonamide complexes structurally characterized so far (Figure 1).[15,24] In particular, the ionized nitrogen atom of the sulfonamide group is coordinated to the zinc ion at a distance of 1.97 Å. This nitrogen is also hydrogen-bonded to the hydroxyl group of Thr199 (N···Thr199OG = 2.74 Å), which in turn interacts with the Glu106OE1 atom (2.54 Å). The inhibitor O1 atom is hydrogen-bonded to the backbone amide of Thr199

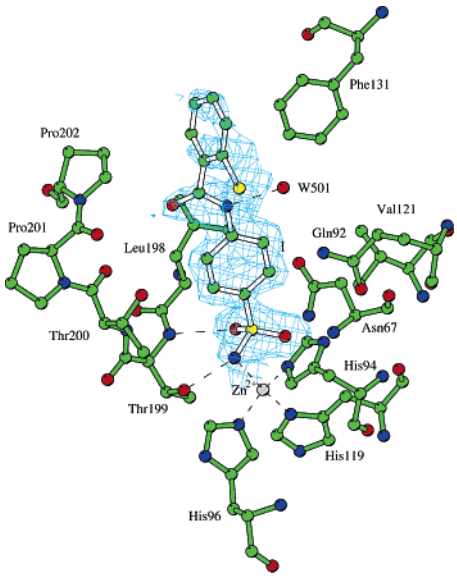

Figure 1. Simulated annealing omit $|2F_o - F_c|$ electron density map contoured at 1.0*σ* for the hCA II−**H5a** adduct. The inhibitor, identified with the "I" label, is shown in the active site region. Hydrogen bonds and the active site Zn^{2+} ion coordination are also shown (dotted lines).

(ThrN···O1 = 2.85 Å), whereas the O2 atom is 2.93 Å from the catalytic Zn^{2+} ion.

An extended network of hydrophobic interactions strongly stabilizes the organic scaffold of the inhibitor within the active site cavity. Thus, the aminocarbonylbenzenesulfonamide moiety of **H5a** fills the active site channel of the enzyme and establishes strong van der Waals interactions (distance of <4.5 Å) with the side chains of Gln92, Val121, Phe131, Leu198, Thr199, Thr200, Pro201, and Pro202 (Figure 1), whereas the **H5a** phenylthio moiety interacts poorly with the enzyme as confirmed by the rather disordered electron density. It is interesting to note that the carboxamido group of the inhibitor does not establish significant polar interactions with the amino acid residues of the active site but is hydrogen-bonded to a water molecule (N2···W501 = 2.68 Å), which in turn interacts with Gln92NE2 atom (Gln92NE2···W501 = 3.35 Å). This interaction has also been observed in the adduct of hCA II with a benzolamide derivative reported earlier by us, in which the secondary sulfonamide moiety (SO_2NH) of the inhibitor was connected to Gln92NE2 by means of a water molecule.[15c]

Modeling Studies. To assess the molecular basis of the small differences observed in the affinity of **H5a** toward hCA II and hCA IX (see Table 1), a model of the adduct of the inhibitor with the tumor-associated isoform hCA IX has been built up by homology modeling and molecular dynamics simulations approaches as described in Experimental Protocols.

The main protein−inhibitor interactions evidenced in this way are schematically depicted in Figure 2. According to this figure, **H5a** presents a spatial arrangement in the hCA IX active site similar to that observed in the complex with isoform II. In particular, the tetrahedral geometry of the Zn^{2+} binding site and the key hydrogen bonds between the sulfonamide moiety of the inhibitor and the enzyme active site were all retained. Even though hCA IX shares only 34% sequence identity with hCA II, residues of isoform II involved in the hydrophobic interactions with the organic scaffold of **H5a** are strictly conserved in the tumor-associated isoform IX except for the mutations Phe131/Val and Asn67/Gln. Thus, all the relevant hydrophobic interactions stabilizing the binding of **H5a** in the hCA II active site are retained in the hCA IX−**H5a** complex. In contrast, a

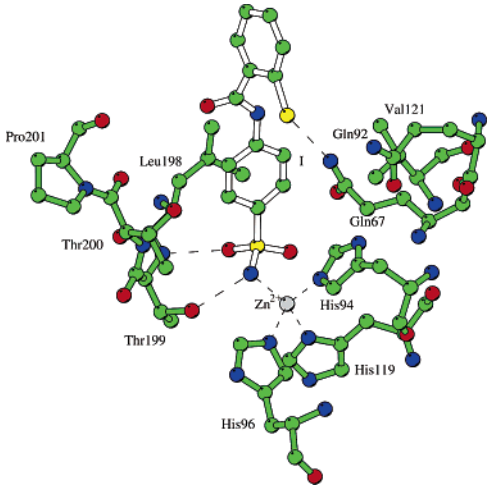

Figure 2. Active site region in the hCA IX−**H5a** complex showing the residues participating in recognition of the inhibitor molecule. Hydrogen bonds and the active site Zn^{2+} ion coordination are also shown (dotted lines).

unique polar interaction distinguishes the hCA IX−**H5a** adduct from its hCA II counterpart. In fact, the mutated Gln67 is involved in the formation of a stable hydrogen bond with the thiol group of **H5a** (Gln67NE2···S2 = 3.2 Å). This weak polar interaction, which is absent in hCA II as a consequence of the shorter side chain of Asn67, can be considered as the unique structural feature accounting for the observed differences in binding affinity of **H5a** toward hCA II and hCA IX, but it is presumably quite important, since this inhibitor is roughly 2 times a more effective inhibitor of the tumor-associated isozyme (hCA IX) over the cytosolic one (hCA II).

Conclusions

We report here a novel approach for the design of bioreductive, hypoxia-activatable CA inhibitors targeting the tumor-associated isoform hCA IX. Sulfonamides incorporating 3,3′-dithiodipropionamide and 2,2′-dithiodibenzamido moieties have been obtained from aminosulfonamides and dithiodi-aliphatic/aromatic acyl halides. Such compounds may be reduced enzymatically (or chemically) under the reducing conditions present in hypoxic tumors, which are also rich in the redox protein thioredoxin-1, known to mediate this type of reduction with formation of thiol derivatives. Since the last compounds are much less bulky than the disulfides, they may show better CA inhibitory activity compared to the bulky, sterically hindered disulfides, which have difficulty entering the limited space of the enzyme active site. Indeed, most disulfides reported here showed this type of behavior, whereas the corresponding thiols acted as potent inhibitors of hCA I, II, and IX (with inhibition constants in the range 3.2−18 nM against the tumor-associated isoform). The X-ray crystal structure of the most promising compound in its reduced form, 4-(2-mercaptophenylcarboxamido)benzenesulfonamide, which as a disulfide showed a K_I against hCA IX of 653 nM (in reduced form of 9.1 nM), in adduct with hCA II showed the inhibitor making a host of favorable interactions with the side chains of Gln92, Val121, Phe131, Leu198, Thr199, Thr200, Pro201, and Pro202, whereas the deprotonated sulfamoyl moiety was coordinated to the Zn^{2+} ion and made the classical hydrogen bonds with Thr199. The same interactions were preserved in the adduct of this compound with hCA IX, but in addition, a hydrogen bond between the SH moiety of the inhibitor and the amide nitrogen of Gln67 was evidenced (which is absent in the hCA II adduct), which may explain the almost 2 times more effective inhibition of the tumor-associated isozyme over the cytosolic isoform. Work is in progress to test the effects of these compounds on their antitumor activity in vivo.

Experimental Protocols

General. ^{1}H NMR spectra were recorded on a Bruker DRX-400 spectrometer using DMSO-d_6 as solvent and tetramethylsilane as internal standard. Chemical shifts are expressed in δ (ppm) downfield from tetramethylsilane, and coupling constants (J) are expressed in hertz. Electron ionization mass spectra (30 eV) were recorded in positive or negative mode on a Water MicroMass ZQ.

General Procedure for the Synthesis of *N,N′*-(Dithiodipropionyl)bis(sulfonamide) Compounds (2−4). An amount of 3 g of dithiodipropionic acid was suspended in $SOCl_2$ (15 mL), and the mixture was refluxed until complete dissolution of the acid. Thionyl chloride was then removed under reduced pressure to yield the dithiodipropionyl dichloride **1** as a pale-yellow oil. Compound **1** was used in the next step without further purification. Dithiodipropionyl dichloride **1** (1equiv, 1.2 mmol) dissolved in dioxane (5 mL) was added in a pyridine solution (10 mL) of aminosulfonamide (3equiv). The mixture was stirred at room temperature for 12 h and then poured into 200 mL of water and filtered. The residue was washed several times with water, dichloromethane, and ether. The corresponding *N,N′*-(dithiodipropionyl)bis(sulfonamides) are obtained as a powder in 60−80% yields.

***N,N′*-(Dithiodipropionyl)bis(4-aminobenzenesulfonamide) 2a:** ^{1}H NMR (DMSO-d_6, 400 MHz) δ 10.40 (s, 2H), 7.76 (m, 8H), 7.26 (s, 4H), 3.03 (m, 4H), 2.80 (m, 4H). MS ESI$^+$ m/z 541 (M + Na)$^+$. Anal. ($C_{18}H_{22}N_4O_6S_4$) C, H, N.

***N,N′*-(Dithiodipropionyl)bis(4-amino-3-fluorobenzenesulfonamide) 2b:** ^{1}H NMR (DMSO-d_6, 400 MHz) δ 9.95 (s, 2H), 8.2 (d, 2H, J = 8 Hz), 7.92 (d, 2H, J = 1.6 Hz), 7.77 (dd, 2H, J = 8.4, 1.6 Hz), 7.50 (s, 4H), 3.05 (t, 4H, J = 6.7 Hz), 2.95 (t, 2H, J = 6.7 Hz). MS ESI$^+$ m/z 577 (M + Na)$^+$. Anal. ($C_{18}H_{20}F_2N_4O_6S_4$) C, H, N.

***N,N′*-(Dithiodipropionyl)bis(4-amino-3-chlorobenzenesulfonamide) 2c:** ^{1}H NMR (DMSO-d_6, 400 MHz) δ 9.91 (s, 2H), 8.0 (d, 2H, J = 8 Hz), 7.89 (d, 2H, J = 1.6 Hz), 7.75 (dd, 2H, J = 8.4 Hz, 1.6 Hz), 7.47 (s, 4H), 3.04 (t, 4H, J = 6.8 Hz), 2.91 (t, 2H, J = 6.8 Hz). MS ESI$^+$ m/z 611 (M + Na)$^+$. Anal. ($C_{18}H_{20}Cl_2N_4O_6S_4$) C, H, N.

***N,N′*-(Dithiodipropionyl)bis(4-aminoethylbenzenesulfonamide) 2d:** ^{1}H NMR (DMSO-d_6, 400 MHz) δ 8.11 (t, 2H, J = 5.6 Hz), 7.74 (d, 4H, J = 8.4 Hz), 7.39 (d, 4H, J = 8.4 Hz), 7.31 (s, 4H), 3.30 (q, 4H, J = 13.2 Hz, 5.2 Hz), 2.88 (t, 4H, J = 7.6 Hz), 2.78 (t, 4H, J = 7.6 Hz), 2.46 (t, 4H, J = 7.2 Hz). MS ESI$^+$ m/z 575 (M + H)$^+$. Anal. ($C_{22}H_{30}N_4O_6S_4$) C, H, N.

***N,N′*-(Dithiodipropionyl)bis(5-amino-1,3,4-thiadiazole-2-sulfonamide) 3:** ^{1}H NMR (DMSO-d_6, 400 MHz) δ 13.1 (s, 2H), 8.35 (s, 4H), 3.05 (t, 4H, J = 6.8 Hz), 2.97 (t, 4H, J = 6.8 Hz). MS ESI$^-$ m/z 533 (M − H)$^-$. Anal. ($C_{10}H_{14}N_8O_6S_6$) C, H, N.

***N,N′*-(Dithiodipropionyl)bis(4-methyl-1,3,4-thiadiaolin-5-ylidene-2-sulfonamide) 4:** ^{1}H NMR (DMSO-d_6, 400 MHz) δ 8.49 (s, 4H), 3.94 (s, 6H), 3.07 (t, 4H, J = 6.5 Hz), 2.94 (t, 4H, J = 6.5 Hz). MS ESI$^+$ m/z 564 (M + H)$^+$. Anal. ($C_{12}H_{19}N_8O_6S_6$) C, H, N.

CA Inhibition Assay. An Applied Photophysics stopped-flow instrument has been used for assaying the CA catalyzed CO_2 hydration activity.[29] Phenol red (at 0.2 mM) was used as indicator, working at the absorbance maximum of 557 nm, with 10 mM Hepes (pH 7.5) as buffer, 0.1 M Na_2SO_4 (for maintaining constant the ionic strength), following the CA-catalyzed CO_2 hydration reaction for 10−15 s. The CO_2 concentrations ranged from 1.7 to 17 mM for the determination of the kinetic parameters and inhibition constants. For each inhibitor at least six traces of the initial 5−10% of the reaction have been used for determining the initial velocity. The uncatalyzed rates were determined in the same manner and subtracted from the total observed rates. Stock solutions of inhibitor (1 mM) were prepared in distilled−deionized water with 10% (v/v) DMSO (which is not inhibitory at these concentrations), and

dilutions up to 0.01 nM were done thereafter with distilled−deionized water. Inhibitor and enzyme solutions were preincubated together for 15 min at room temperature prior to assay, to allow for the formation of the E−I complex. The inhibition constants were obtained by nonlinear least-squares methods from Lineweaver−Burk plots, as reported earlier,[12−15] and represent the mean of at least three different determinations.

Crystallization, X-ray Data Collection, and Refinement. The hCA II−**H5a** complex was obtained by adding a 5 M excess of compound **5a** to a 10 mg/mL protein solution in 100 mM Tris-HCl, pH 8.5. Crystals of the complex were obtained using the hanging drop vapor diffusion technique. The drop consisted of 2 μL of the complex solution and 2 μL of the precipitant solution containing 2.5 M $(NH_4)_2SO_4$, 0.3 M NaCl, 100 mM Tris-HCl (pH 8.2), and 5 mM 4-(hydroxymercurybenzoate) to improve the crystal quality. Crystals appeared after 1 week at 18 °C. X-ray diffraction data were collected at synchrotron source Elettra in Trieste, using a Mar CCD detector at 100 K. A cryoprotectant solution was made by inclusion of 15% (v/v) glycerol in the reservoir solution. Data were measured to 1.80 Å resolution and processed using Denzo.[32] A total of 68 934 reflections were measured and reduced to 21 376 unique reflections (Table 2). The structure of the complex was analyzed by difference Fourier techniques, using the PDB file 1CA2[30] as a starting model for refinement. Water molecules were removed from the starting model prior to structure factor and phase calculations. The crystallographic R factor and R_{free}, calculated in the 20.00−1.80 Å resolution range and based on the starting model coordinates, were 0.368 and 0.353, respectively. Clear electron density for only one monomeric unit (obtained by the reduction of the disulfide bond present in **5a**, with formation of **H5a**; Scheme 2) of the inhibitor was observed in the difference map after a single round of refinement (R factor of 0.253 and R_{free} of 0.288). A model for the inhibitor was then easily built and introduced into the atomic coordinates set for further refinement, which proceeded to convergence with alternating cycles of water addiction, manual rebuilding with the O program,[33] and energy minimization and B-factor refinement with the CNS program.[31] The final crystallographic R factor and R_{free} values calculated for the 21 029 observed reflections (in the 20.00−1.80 Å resolution range) were 0.184 and 0.218, respectively. The statistics for refinement are summarized in Table 2. Coordinates and structure factors have been deposited in the Brookhaven Protein Data Bank (accession code 2HD6).

Modeling Studies and Molecular Dynamics Simulations. A model of hCA IX catalytic domain was obtained using both hCA II and mCA XIV X-ray structures as templates as previously described by Alterio et al.[34] The hCA IX−**H5a** starting adduct was then derived by superimposing the three histidine residues coordinating the Zn^{2+} active site ion of hCA II− **H5a** X-ray structure onto corresponding atoms of the hCA IX model. This preliminary adduct model was further completed by addition of all hydrogen atoms and underwent energy minimization with the SANDER module of AMBER8 package[35] using the PARM99 force field.[36]

Atomic charges of the **H5a** molecule were obtained with RESP methodology.[37] The **H5a** conformation derived from the hCA II−**H5a** crystal structure was fully optimized using the GAMESS program[38] at the Hartree−Fock level with the STO-3G basis set. Single-point calculations on optimized molecule was performed at the RHF/6-31G* level. The resulting electrostatic potential was thus used for a one-stage single-conformation RESP charge fitting. Partial charges for the three catalytic histidines and Zn^{2+} were those published by Suarez and Merz.[39] To preserve the integral charge of the whole system, partial charges of Cα and Hα atoms of the Zn^{2+}−ligand residues and of N and H atoms of the inhibitor sulfonamide group were modified accordingly. A bonded approach between the Zn^{2+} ion and its ligands was adopted to preserve the experimentally observed tetrahedral Zn^{2+} coordination in all complexes during MD simulations. Equilibrium bond distances and bond angles involving the Zn^{2+} ion were derived from the hCA II−**H5a** crystal structure. Force constants of 120 kcal mol^{-1} Å^{-1} were used for N(His)−Zn^{2+} bond parameters, while force constants of 20 and 30 kcal mol^{-1} Å^{-1} were adopted for N(His)− Zn^{2+}−N(His) and N(His)−Zn−N(sulfonamide) angle parameters, respectively. All the torsional parameters associated with interactions between Zn^{2+} and its ligands were set to zero as in Hoops et al.[40] To perform MD simulations in solvent, minimized models were confined in truncated octahedral boxes filled with TIP3P water molecules and counterions (Na^+) to ensure electrostatic neutrality. The solvated molecules were then energy-minimized through 1000 steps with solute atoms restrained to their starting positions, using a force constant of 10 kcal mol^{-1} Å^{-1} prior to MD simulations. The molecules were then submitted to 90 ps of restrained MD (5 kcal mol^{-1} Å^{-1}) at constant volume, gradually being heated to 300 K, followed by 60 ps of restrained MD (5 kcal mol^{-1} Å^{-1}) at constant pressure to adjust system density. MD production runs were carried out at 300 K for 1 ns with a time step of 1.5 fs. Bonds involving hydrogens were constrained using the SHAKE algorithm.[41] Snapshots from production runs were saved every 1000 steps and analyzed with MOLMOL program.[42]

Acknowledgment. This work was financed in part by an EU grant of the 6th Framework Programme (EUROXY project). We thank the Sincrotrone Trieste CNR/Elettra for giving us the opportunity to collect data at the crystallographic beamline.

Supporting Information Available: Elemantal analysis results of compounds **2**−**4**. This material is available free of charge via the Internet at http://pubs.acs.org.

References

(1) Pastorekova, S.; Pastorek, J. Cancer-Related Carbonic Anhydrase Isozymes. In *Carbonic Anhydrase. Its Inhibitors and Activators*; Supuran, C. T., Scozzafava, A., Conway, J., Eds.; CRC Press: Boca Raton, FL, 2004; pp 253−280.

(2) (a) Supuran, C. T.; Scozzafava, A.; Casini, A. Carbonic anhydrase inibitors. *Med. Res. Rev.* **2003**, *23*, 146−189. (b) Supuran, C. T., Scozzafava, A., Conway, J., Eds. *Carbonic Anhydrase. Its Inhibitors and Activators*; CRC Press (Taylor and Francis Group): Boca Raton, FL, 2004; pp 1−363 and references therein. (c) Casini, A.; Scozzafava, A.; Mastrolorenzo, A.; Supuran, C. T. Sulfonamides and sulfonylated derivatives as anticancer agents. *Curr. Cancer Drug Targets* **2002**, *2*, 55−75.

(3) (a) Wykoff, C. C.; Beasley, N. J.; Watson, P. H.; Turner, K. J.; Pastorek, J.; Sibtain, A.; Wilson, G. D.; Turley, H.; Talks, K. L.; Maxwell, P. H.; Pugh, C. W.; Ratcliffe, P. J.; Harris, A. L. Hypoxia-inducible regulation of tumor-associated carbonic anhydrases. *Cancer Res.* **2000**, *60*, 7075−7083. (b) Potter, C. P. S.; Harris, A. L. Diagnostics, prognostics and therapeutic implications of carbonic anhydrases in cancer. *Br. J. Cancer* **2003**, *89*, 2−7. (c) Jain, R. K. Normalization of tumor vasculature: an emerging concept in antiangiogenic therapy. *Science* **2005**, *307*, 58−62.

(4) (a) Pastorek, J.; Pastorekova, S.; Callebaut, I.; Mornon, J. P.; Zelnik, V.; Opavsky, R.; Zatovicova, M.; Liao, S.; Portetelle, D.; Stanbridge, E. J.; Zavada, J.; Burny, A.; Kettmann, R. Cloning and characterization of MN, a human tumor-associated protein with a domain homologous to carbonic anhydrase and a putative helix−loop−helix DNA binding segment. *Oncogene* **1994**, *9*, 2788−2888. (b) Opavský, R.; Pastorekova, S.; Zelnik, V.; Gibadulinova, A.; Stanbridge, E. J.; Zavada, J.; Kettmann, R.; Pastorek, J. Human MN/CA9 gene, a novel member of the carbonic anhydrase family: structure and exon to protein domain relationship. *Genomics* **1996**, *33*, 480−487.

(5) Maxwell, P. H.; Wiesener, M. S.; Chang, G. W.; Clifford, S. C.; Vaux, E. C.; Cockman, M. E.; Wykoff, C. C.; Pugh, C. W.; Maher, E. R.; Ratcliffe, P. J. The tumour suppressor protein VHL targets hypoxia-inducible factors for oxygen-dependent proteolysis. *Nature* **1999**, *399*, 271−275.

(6) Epstein, A. C. R.; Gleadle, J. M.; McNeil, L. A. *C. elegans* EGL-9 and mammalian homologs define a family of dioxygenases that regulate HIF by prolyl hydroxylation. *Cell* **2001**, *107*, 43−54

(7) Ratcliffe, P. J.; Pugh, C. W.; Maxwell, P. H. Targeting tumors through the HIF system. *Nat. Med.* **2000**, *6*, 1315−1316.

(8) Jaakkola, P.; Mole, D. R.; Tian, Y. M.; Wilson, M. I.; Gielbert, J.; Gaskell, S. J.; Kriegsheim, A. V.; Hebestreit, H. F.; Mukherji, M.; Schofield, C. J.; Maxwell, P. H.; Pugh, C. W.; Ratcliffe, P. J. Targeting of HIF-α to the von Hippel Lindau ubiquitilation complex by O_2-regulated prolyl hydroxylation. *Science* **2001**, *292*, 468−472.

(9) Harris, AL. Hypoxia, a key regulatory factor in tumour growth. *Nat. Rev. Cancer* **2002**, *2*, 38−47.

(10) Semenza, G. L. Targeting HIF-1 for cancer therapy. *Nat. Rev. Cancer* **2003**, *3*, 721−732.
(11) Svastova, E.; Hulikova, A.; Rafajova, M.; Zatovicova, M.; Gibadulinova, A.; Casini, A.; Cecchi, A.; Scozzafava, A.; Supuran, C. T.; Pastorek, J.; Pastorekova, S. Hypoxia activates the capacity of tumor-associated carbonic anhydrase IX to acidify extracellular pH. *FEBS Lett.* **2004**, *577*, 439−445.
(12) (a) Cecchi, A.; Hulikova, A.; Pastorek, J.; Pastorekova, S.; Scozzafava, A.; Winum, J.-Y.; Montero, J.-L.; Supuran, C. T. Carbonic anhydrase inhibitors. Sulfonamides inhibit isozyme IX mediated acidification of hypoxic tumors. Fluorescent sulfonamides design as probes of membrane-bound carbonic anhydrase isozymes involvement in tumorigenesis. *J. Med. Chem.* **2005**, *48*, 4834−4841. (b) Casey, J. R.; Morgan, P. E.; Vullo, D.; Scozzafava, A.; Mastrolorenzo, A.; Supuran, C. T. Carbonic anhydrase inhibitors. Design of selective, membrane-impermeant inhibitors targeting the human tumor-associated isozyme IX. *J. Med. Chem.* **2004**, *47*, 2337−2347.
(13) Vullo, D.; Franchi, M.; Gallori, E.; Pastorek, J.; Scozzafava, A.; Pastorekova, S.; Supuran, C. T. Carbonic anhydrase inhibitors. Inhibition of the tumor-associated isozyme IX with aromatic and heterocyclic sulfonamides. *Bioorg. Med. Chem. Lett.* **2003**, *13*, 1005−1009.
(14) (a) Pastorekova, S.; Casini, A.; Scozzafava, A.; Vullo, D.; Pastorek, J.; Supuran, C. T. Carbonic anhydrase inhibitors: The first selective, membrane-impermeant inhibitors targeting the tumor-associated isozyme IX. *Bioorg. Med. Chem. Lett.* **2004**, *14*, 869−873. (b) Winum, J. Y.; Scozzafava, A.; Montero, J. L.; Supuran, C. T. Sulfamates and their therapeutic potential. *Med. Res. Rev.* **2005**, *25*, 186−228. (c) Winum, J. Y.; Scozzafava, A.; Montero, J. L.; Supuran, C. T. The sulfamide motif in the design of enzyme inhibitors. *Expert Opin. Ther. Pat.* **2006**, *16*, 27−47.
(15) (a) Abbate, F.; Casini, A.; Owa, T.; Scozzafava, A.; Supuran, C. T. Carbonic anhydrase inhibitors: E7070, a sulfonamide anticancer agent, potently inhibits cytosolic isozymes I and II, and transmembrane, tumor-associated isozyme IX. *Bioorg. Med. Chem. Lett.* **2004**, *14*, 217−223. (b) Weber, A.; Casini, A.; Heine, A.; Kuhn, D.; Supuran, C. T.; Scozzafava, A.; Klebe, G. Unexpected nanomolar inhibition of carbonic anhydrase by COX-2 selective Celecoxib: New pharmacological opportunities due to related binding site recognition. *J. Med. Chem.* **2004**, *47*, 550−557. (c) Abbate, F.; Casini, A.; Scozzafava, A.; Supuran, C. T. Carbonic anhydrase inhibitors: X-ray crystallographic structure of the adduct of human isozyme II with a topically acting antiglaucoma sulfonamide. *Bioorg. Med. Chem. Lett.* **2004**, *14*, 2357−2361.
(16) Supuran, C. T.; Briganti, F.; Tilli, S.; Chegwidden, W. R.; Scozzafava, A. Carbonic anhydrase inhibitors: Sulfonamides as antitumor agents? *Bioorg. Med. Chem.* **2001**, *9*, 703−714.
(17) Parkkila, S.; Rajaniemi, H.; Parkkila, A. K.; Kivela, J.; Waheed, A.; Pastorekova, S.; Pastorek, J.; Sly, W. S. Carbonic anhydrase inhibitor suppresses invasion of renal cancer cells in vitro. *Proc. Natl. Acad. Sci. U.S.A.* **2000**, *97*, 2220−2224.
(18) Pastorekova, S.; Parkkila, S.; Pastorek, J.; Supuran C. T. Carbonic anhydrases: current state of the art, therapeutic applications and future prospects. *J. Enzyme Inhib. Med. Chem.* **2004**, *19*, 199−229.
(19) (a) Denny, W. A. Tumor-activated prodrugs. A new approach to cancer therapy. *Cancer Invest.* **2004**, *22*, 604−619. (b) Stratford, I. J.; Williams, K. J.; Cowen, R. L.; Jaffar, M. Combining bioreductive drugs and radiation for the treatment of solid tumors. *Semin. Radiat. Oncol.* **2003**, *13*, 42−52. (c) Frein, D.; Schildknecht, S.; Bachschmid, M.; Ullrich, V. Redox regulation: a new challenge for pharmacology. *Biochem. Pharmacol.* **2005**, *70*, 811−823. (d) Garber, K. New drugs target hypoxia response in tumors. *J. Natl. Cancer Inst.* **2005**, *97*, 1112−1114.
(20) Hay, M. P.; Pruijn, F. B.; Gamage, S. A.; Liyanage, H. D.; Kovacs, M. S.; Patterson, A. V.; Wilson, W. R.; Brown, J. M.; Denny, W. A. DNA-targeted 1,2,4-benzotriazine 1,4-dioxides: potent analogues of the hypoxia-selective cytotoxin tirapazamine. *J. Med. Chem.* **2004**, *47*, 475−488.
(21) Seow, H. A.; Penketh, P. G.; Shyam, K.; Rockwell, S.; Sartorelli, A. C. 1,2-Bis(methylsulfonyl)-1-(2-chloroethyl)-2-[[1-(4-nitrophenyl)-ethoxy]carbonyl]hydrazine: an anticancer agent targeting hypoxic cells. *Proc. Natl. Acad. Sci. U.S.A.* **2005**, *102*, 9282−9287.
(22) Nomura, M.; Shuto, S.; Matsuda, A. Synthesis of the cyclic and acyclic acetal derivatives of 1-(3-C-ethynyl-beta-D-ribo-pentofuranosyl)cytosine, a potent antitumor nucleoside. Design of prodrugs to be selectively activated in tumor tissues via the bio-reduction−hydrolysis mechanism. *Bioorg. Med. Chem.* **2003**, *11*, 2453−2461.
(23) Phillips, R. M.; Jaffar, M.; Maitland, D. J.; Loadman, P. M.; Shnyder, S. D.; Steans, G.; Cooper, P. A.; Race, A.; Patterson, A. V.; Stratford, I. J. Pharmacological and biological evaluation of a series of substituted 1,4-naphthoquinone bioreductive drugs. *Biochem. Pharmacol.* **2004**, *68*, 2107−2116.
(24) (a) Supuran, C. T.; Scozzafava, A.; Casini, A. Carbonic anhydrase inhibitors. *Med. Res. Rev.* **2003**, *23*, 146−89. (b) Supuran, C. T.; Scozzafava, A.; Casini, A., Development of Sulfonamide Carbonic Anhydrase Inhibitors. In *Carbonic Anhydrase. Its Inhibitors and Activators*; Supuran, C. T., Scozzafava, A., Conway, J., Eds.; CRC Press: Boca Raton, FL, 2004; pp 67−147.
(25) Welsh, S. J.; Williams, R. R.; Birmingham, A.; Newman, D. J.; Kirkpatrick, D. L.; Powis, G. The thioredoxin redox inhibitors 1-methylpropyl 2-imidazolyl disulfide and pleurotin inhibit hypoxia-induced factor 1-alpha and vascular endothelial growth factor formation. *Mol. Cancer Ther.* **2003**, 2, 235−243.
(26) (a) Scozzafava, A.; Menabuoni, L.; Mincione, F.; Briganti, F.; Mincione, G.; Supuran, C. T. Carbonic anhydrase inhibitors. Synthesis of water-soluble, topically effective, intraocular pressure-lowering aromatic/heterocyclic sulfonamides containing cationic or anionic moieties: is the tail more important than the ring? *J. Med. Chem.* **1999**, *42*, 2641−2650. (b) Winum, J. Y.; Dogne, J. M.; Casini, A.; de Leval, X.; Montero, J. L.; Scozzafava, A.; Vullo, D.; Innocenti, A.; Supuran, C. T. Carbonic anhydrase inhibitors: synthesis and inhibition of cytosolic/membrane-associated carbonic anhydrase isozymes I, II, and IX with sulfonamides incorporating hydrazino moieties. *J. Med. Chem.* **2005**, *48*, 2121−2125.
(27) Turpin, J. A.; Song, Y.; Inman, J. K.; Huang, M.; Wallqvist, A.; Maynard, A.; Covell, D. G.; Rice, W. G.; Appella, E. Synthesis and biological properties of novel pyridinioalkanoyl thiolesters (PATE) as anti-HIV-1 agents that target the viral nucleocapsid protein zinc fingers. *J. Med. Chem.* **1999**, *42*, 67−86.
(28) (a) Innocenti, A.; Vullo, D.; Scozzafava, A.; Supuran, C. T. Carbonic anhydrase inhibitors. Inhibition of isozymes I, II, IV, V and IX with anions isosteric and isoelectronic with sulfate, nitrate and carbonate. *Bioorg. Med. Chem. Lett.* **2005**, *15*, 567−571. (b) Vullo, D.; Franchi, M.; Gallori, E.; Pastorek, J.; Scozzafava, A.; Pastorekova, S.; Supuran, C. T. Carbonic anhydrase inhibitors. Inhibition of cytosolic isozymes I and II and transmembrane, cancer-associated isozyme IX with anions. *J. Enzyme Inhib. Med. Chem.* **2003**, *18*, 403−406.
(29) Khalifah, R. G. The carbon dioxide hydration activity of carbonic anhydrase. I. Stop-flow kinetic studies on the native human isoenzymes B and C. *J. Biol. Chem.* **1971**, *246*, 2561−2573.
(30) Eriksson, A. E.; Jones, T. A.; Liljas, A. Refined structure of human carbonic anhydrase II at 2.0 Å resolution. *Proteins: Struct., Funct., Genet.* **1988**, *4*, 274−282.
(31) Brünger, A. T.; Adams, P. D.; Clore, G. M.; De Lano, W. L.; Gros, P.; Grosse-Kunstleve, R. W.; Jiang, J. S.; Kuszewski, J.; Nilges, M.; Pannu, N. S.; Read, R. J.; Rice, L. M.; Simonson, T.; Warren, G. L. Crystallography & NMR system: A new software suite for macromolecular structure determination. *Acta Crystallogr., Sect. D: Biol. Crystallogr.* **1998**, *54*, 905−921.
(32) Otwinowski, Z.; Minor, W. Processing of X-ray diffraction data collected in oscillation mode. *Methods Enzymol.* **1997**, *276*, 307−326.
(33) Jones, T. A.; Zou, J. Y.; Cowan, S. W.; Kjeldgaard, M. Improved methods for building protein models in electron density maps and the location of errors in these models. *Acta Crystallogr., Sect. A* **1991**, *47*, 110−119.
(34) Alterio, V.; Vitale, R. M.; Monti, S. M.; Pedone, C.; Scozzafava, A.; Cecchi, A.; De Simone, G.; Supuran, C. T. Carbonic anhydrase inhibitors: X-ray and molecular modeling study for the interaction of a fluorescent antitumor sulfonamide with isozyme II and IX. *J. Am. Chem. Soc.* **2006**, *128*, 8329−8335.
(35) Pearlman, D. A.; Case, D. A.; Caldwell, J. W.; Ross, W. S.; Cheatham, T. E., III.; DeBolt, S.; Ferguson, D.; Seibel, G.; Kollman, P. "AMBER", a package of computer programs for applying molecular mechanics, normal mode analysis, molecular dynamics and free energy calculations to simulate the structural and energetic properties of molecules. *Comput. Phys. Commun.* **1995**, *91*, 1−42.
(36) Wang, J.; Cieplak, P.; Kollman, P. A. How well does a restrained electrostatic potential (RESP) model perform in calculating conformational energies of organic and biological molecules? *J. Comput. Chem.* **2000**, *21*, 1049−1074.
(37) Bayly, C. I.; Cieplak, P.; Cornell, W.; Kollman, P. A. A well-behaved electrostatic potential based method using charge restraints for deriving atomic charges: the RESP model. *J. Phys. Chem.* **1993**, *97*, 10269−10280.
(38) Schmidt, M. W.; Baldridge, K. K.; Boatz, J. A.; Elbert, S. T.; Gordon, M. S.; Jensen, J. H.; Koseki, S.; Matsunaga, N.; Nguyen, K. A. General atomic and molecular electronic structure system. *J. Comput. Chem.* **1993**, *14*, 1347−1363.
(39) Suarez, D.; Merz, K. M., Jr. Molecular dynamics simulations of the mononuclear zinc-beta-lactamase from *Bacillus cereus*. *J. Am. Chem. Soc.* **2001**, *123*, 3759−3770.

(40) Hoops, S. C.; Anderson, K. W.; Merz, K. M., Jr. Force field design for metalloproteins. *J. Am. Chem. Soc*. **1991**, *113*, 8262−8270.
(41) Ryckaert, J. P.; Ciccotti, G.; Berendsen, H. J. Numerical integration of the Cartesian equations of motion of a system with constraints: molecular dynamics of *n*-alkanes. C. *J. Comput. Phys.* **1977**, *23*, 327−341.
(42) Koradi, R.; Billeter, M.; Wuethrich, K. MOLMOL: a program for display and analysis of macromolecular structures. *J. Mol. Graphics* **1996**, *14*, 51−55, plates 29−32.

JM060531J